

Investigation into laser sintering of PEEK using commercially available low powder bed temperature machine

Takashi KIGURE*, Yuki YAMAUCHI*, Toshiki NIINO†

*Tokyo Metropolitan Industrial Technology Research Institute

†Institute of Industrial Science, the University of Tokyo

Abstract

Polyetheretherketone (PEEK) is one of the highest performance plastics in terms of heat and chemical resistance and mechanical strength. Laser sintering of PEEK requires high powder bed temperature above 300°C, and this pushes up machine price and pulls down powder recycle rate which leads to high material cost.

The authors are proposing a modified laser sintering process which allows the bed temperature to be set lower than recrystallization temperature, namely low temperature process. In this research, bed temperature of 170 °C, which is typical for PA12 process, and bed temperature of 200 °C which is same as previous study were tested. As a result, parts with a high relative density of more than 95% were obtained at both powder bed temperatures, and parts with a tensile strength of 80 MPa were obtained at a powder bed temperature of 170 °C. This shows that laser sintering of PEEK can be processed with a commercially available laser sintering machine resulting in drastic cost cut in terms of machine and material costs.

Introduction

Recently, laser sintering has been recognized as a manufacturing technology. The material used for laser sintering is mostly PA12, but there is also request for other materials. For example, Polyetheretherketone (PEEK) which is one of the highest-performance plastics in terms of heat, chemical resistance and mechanical strength is one of the requested materials. PEEK is available for laser sintering process, and there are several reports about laser sintering of PEEK.

Beretta et al. attempted prediction of optimal process parameters from powder properties in laser sintering of PEEK. They showed stable sintering region that indicate temperature range of achieving particle fully melting without material thermal degradation [1]. Wanger et al. proposed process to control absorption of laser energy by mixing absorber with material powder and this process was applied for PEEK [2]. Kroh et al. reported that applying post sintering in the Wanger's process resulted in the same strength and modulus as injection molded PEEK [3]. Hopkinsons et al. investigated mechanical properties of commercial used high performance plastics for laser sintering, EOS PEEK HP3. They showed mechanical properties other than elongation at break of laser sintered EOS PEEK HP3 was equivalent to injection molded PEEK [4]. Peyre et al. reported the thermal degradation threshold of PEKK, the same Polyaryletherketone family as PEEK, by a numerical approach and showed that this method helps in the selection of optimal fusion depth parameters [5].

However, laser sintering of PEEK requires high powder bed temperature above 300 °C, and this pushes up machine price and pulls down powder recycle rate which leads to high material cost.

The authors are proposing modified laser sintering process, namely low-temperature process, that suppresses warpage during process by anchoring part to the rigid plate, such as a metal powder bed fusion [6]. This process allows powder bed temperature to be set lower than recrystallization temperature [7]. We have succeeded in improvement of material recycle rate by using this process [8]. Uehara and Niino have succeed laser sintering of PEEK at powder bed temperature of 200 °C and achieved high relative density and strength [9].

But 200 °C is higher than melting temperature of PA12 which is the most popular material in laser sintering. Assuming that PA12 and PEEK are used on the same machine, there is a risk of machine trouble due to residual PA12 when PEEK is used at 200 °C. This risk can be avoided by performing process of PEEK at the same temperature as PA12, and this temperature is suitable for all commercially available laser sintering machines.

The purpose of this study is to show that the most of commercially available machine can be used for PEEK process. In the first step, process at powder bed temperature of 200 °C, which is reported in previous study by experimental machine, was performed. Next, process with powder bed temperature of 170 °C which is same temperature in PA12 process was attempted. Density and mechanical properties of build parts were compared with injection molding and applicability was discussed.

Material and machine

Employed material is PEEK powder, VESTAKEEP® 2000FP (EVONIK). The powder is sieved to remove large grains. Figure1 shows particle distribution of after sieving. The average particle size D50 was 66 μm. Figure 2 shows the Differential Scanning Calorimeter (DSC) curve that indicates thermal properties of this material. The melting point, recrystallization temperature and glass transition temperature are 343 °C, 299 °C and about 150 °C, respectively. Material properties of this PEEK powder is summarized in Table 1.

Modified commercial laser sintering machine RaFaEl300C® was employed in this study. This machine is equipped with CO₂ laser. The laser spot diameter on the powder bed surface is increased to 820 μm by defocusing.

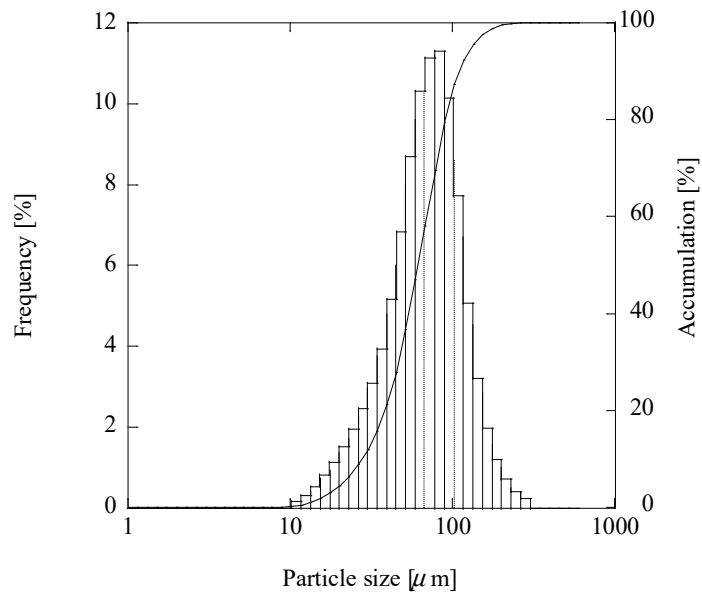


Figure 1. Particle distribution of employed PEEK powder

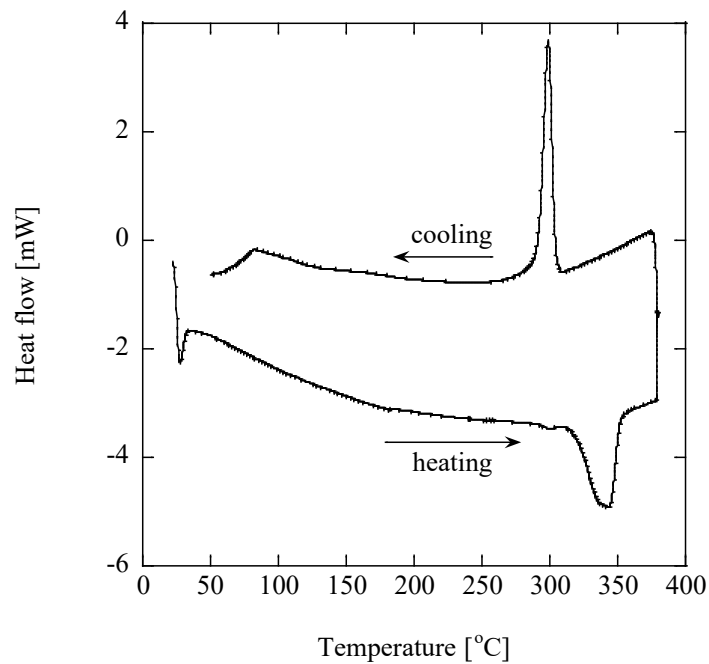


Figure 2. DSC Curve of employed PEEK powder

Table 1. Material properties

Melting temperature	Recrystallization temperature	Glass transition temperature	Ture density	Average particle size (D50)
343 °C	299 °C	approx. 150 °C	1.3 g/cm ³	66 μm

Process condition and evaluation method

Process parameters

Table2 shows manufacturing parameters set. Energy per unit area is defined by follows.

$$\text{Energy per unit area} = \frac{\text{Laser power}}{\text{Scan speed} \times \text{Scan interval}}$$

The powder bed temperature during the process was set to 200 °C and 170 °C, which are lower than the recrystallization temperature. 200°C is the same temperature as in previous experimental studies [9], and 170 °C is equivalent to the powder bed temperature of the PA12 process. Scanning strategy was raster scan and scanning direction was only longitudinal of specimen. Not outline scan was performed.

Table2. Manufacturing parameters set

Powder bed temp.	Layer thickness	Scan speed	Scan Interval	Laser Power	Energy per unit area
200 °C	0.05mm	5 m/s	0.04 mm	30 W, 40 W	0.150 J/mm ² , 0.200 J/mm ²
	0.07mm			30 W-50 W	0.150 J/mm ² – 0.250 J/mm ²
170° C	0.05mm			35 W-50 W	0.175 J/mm ² – 0.250 J/mm ²
	0.07mm			35 W-50 W	0.175 J/mm ² – 0.250 J/mm ²

Building layout

Building layout is shown in Figure 3. 24 half scale test specimen A12 conforming to ISO 20753 were built in one process. One build parameters set was applied every 6 specimens. The specimens were anchored in rigid base plate by support structure. The base plate is made of same material as the specimen.

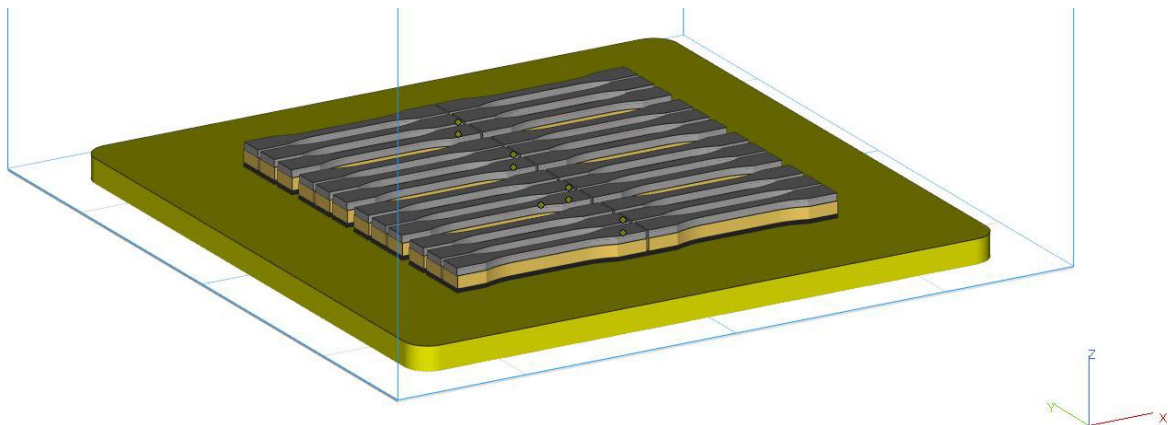


Figure 3. Building layout

Density measuring

Relative density and mechanical properties were measured to evaluate manufactured parts. Relative density was calculated by below. Bulk density of manufactured specimen was measured by Archimedes method.

$$\text{Relative density} = \frac{\text{Bulk density of manufactured specimen}}{\text{Material true density}} \times 100 \%$$

Tensile test

Mechanical properties, such as tensile strength, elastic modulus, and elongation at break, was measured by tensile test. Tensile test was performed Instron® 3365 mechanical testing system (Instron). Cross head speed was set at 0.5 mm per minute from 0 % to 0.25 % strain, which is the measurement range of elastic modulus, and then 2mm per minute until fracture. The elastic modulus was measured by 2630-102 strain gauge extensometer (gauge length 10mm) (Instron) attached to the specimen.

Result

Relative density

Figure 4 shows the specimen removed from the base plate and anchor support. There was almost no warpage of the specimen. Similar trends were seen in the specimens of all build conditions in this study. Figure 5 shows relationship between energy per unit area and relative density. Error bars indicate standard deviation. Relative density increased with increasing laser power in all combinations of powder bed temperature and layer thickness. Except for the combination of powder bed temperature of 200 °C and layer thickness of 0.07 mm, the peak value of relative density exceeded 95%. The relative density shifted higher as the powder bed temperature increased or the layer thickness decreased.



Figure 4. Specimen manufactured in powder bed temperature at 170 °C and layer thickness 0.05mm, energy per unit area of 0.175 J/mm²

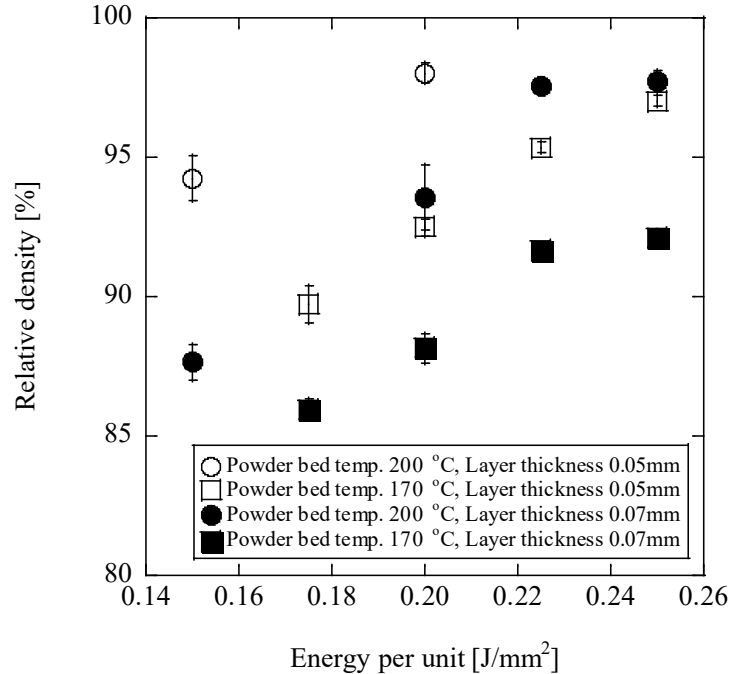


Figure 5. Relationship between relative density and energy per unit area.

Tensile test result

Figure 6 to 8 show relationships between energy per unit area and mechanical properties obtained by tensile test, respectively. Error bar shows standard deviation in all diagrams. Tensile strength is shown in Figure 6. At a powder bed temperature of 170 °C, the tensile strength decreased with an energy per unit area of 0.250 J/mm², and at a powder bed temperature of 200 °C, the tensile strength decreased with energy per unit area of over 0.225 J/mm². The Highest value was shown 80 MPa under energy per unit area at 0.225J/mm² in combination of powder bed temperature 170 °C and layer thickness 0.05 mm.

Elastic modulus is shown in Figure 7. The results with layer thickness 0.05 mm were higher than result with layer thickness 0.07 mm in both powder bed temperature. In all combination of powder bed temperature and layer thickness, values of elastic modulus decreased at energy per unit area of 0.250J/mm². The highest value was about 3100 MPa which was shown in combination of powder bed temperature at 170°C and layer thickness 0.05mm.

Elongation at breaks is shown in Figure 8. Wide error bar shows a wide distribution of results. The highest value of elongation at break was around 6 %. Combination of powder bed temperature at 170 °C and layer thickness 0.05mm showed high value, but clear correlation elongation at break and layer thickness or powder bed temperature was not observed. Table 3 shows summarized of mechanical properties of obtained by tensile test.

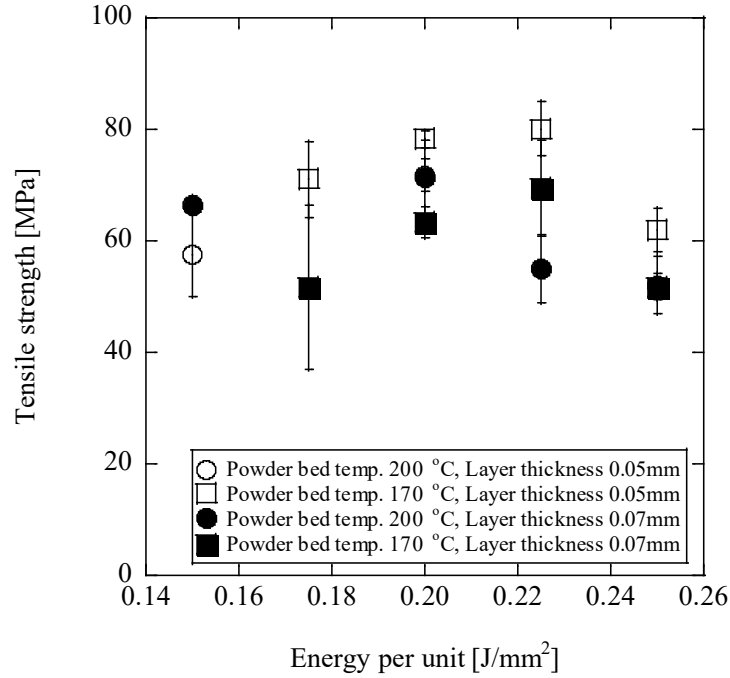


Figure 6. Relationships between tensile strength and energy per unit area.

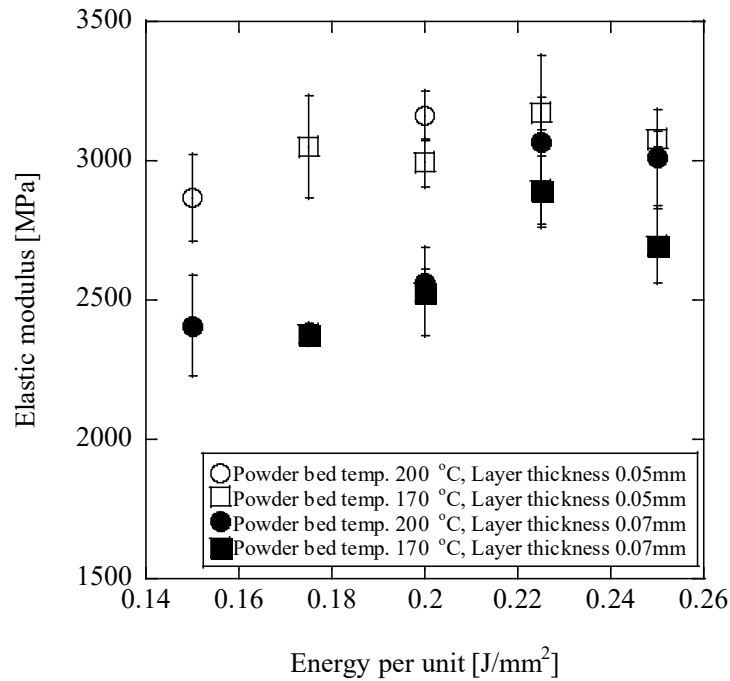


Figure 7. Relationship between elastic modulus and energy pr unit area.

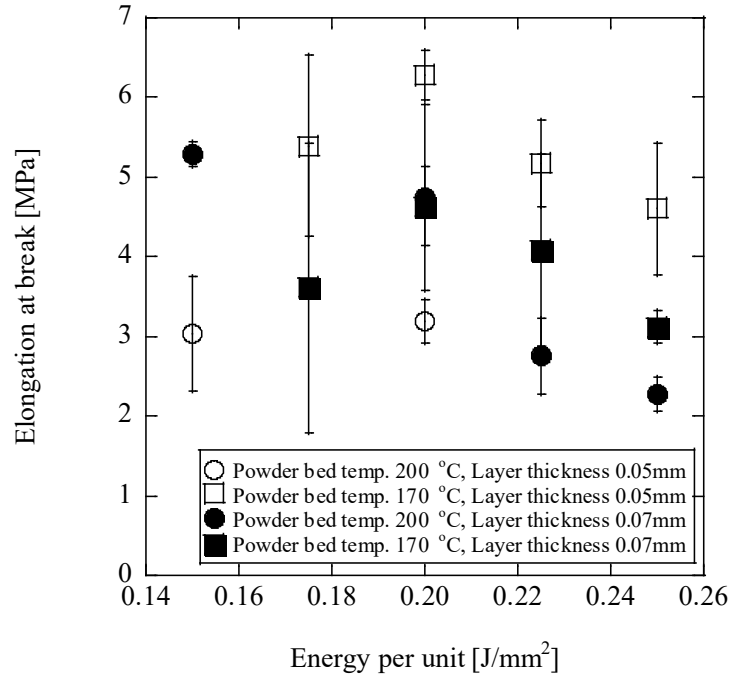


Figure 8. Relationships between elongation at break and energy per unit area.

Table 3. Mechanical properties under conditions with the highest tensile strength

Powder bed temp.	Layer thickness	Energy per unit are	Relative density	Tensile strength	Elastic modulus	Elongation at break
170°C	0.05 mm	0.225 J/mm ²	95.3 ± 0.2 %	80.0 ± 4.9 MPa	3170.1 ± 57.4 MPa	5.2 ± 0.5 %
	0.07 mm	0.225 J/mm ²	91.7 ± 0.2 %	69.6 ± 120.1 MPa	2895.4 ± 120.1 MPa	4.1 ± 1.2 %
200°C	0.05 mm	0.200 J/mm ²	93.6 ± 1.2 %	71.4 ± 6.7 MPa	2558.8 ± 52.0 MPa	4.7 ± 1.2 %
	0.07 mm	0.200 J/mm ²	98.0 ± 0.4 %	71.7 ± 2.9 MPa	3161.0 ± 88.4 MPa	3.2 ± 0.3 %
Injection Mold [12]	-	-	-	100 MPa	3700 MPa	30 %

Figure 9 and Figure 10 shows typical stress-strain curve for each build parameters set. The solid line indicated layer thickness 0.05 mm and dot line indicated layer thickness 0.07 mm, in both graphs. Yield and plastic behavior were observed in curves that have over 60MPa fracture stress. curves Especially, in powder bed temperature 170 °C and layer thickness 0.05mm, clear yield and plastic behavior were observed except for energy per unit area 0.250J/mm². On the other hand, curves that fracture stress was below 60 MPa were shown brittle behavior.

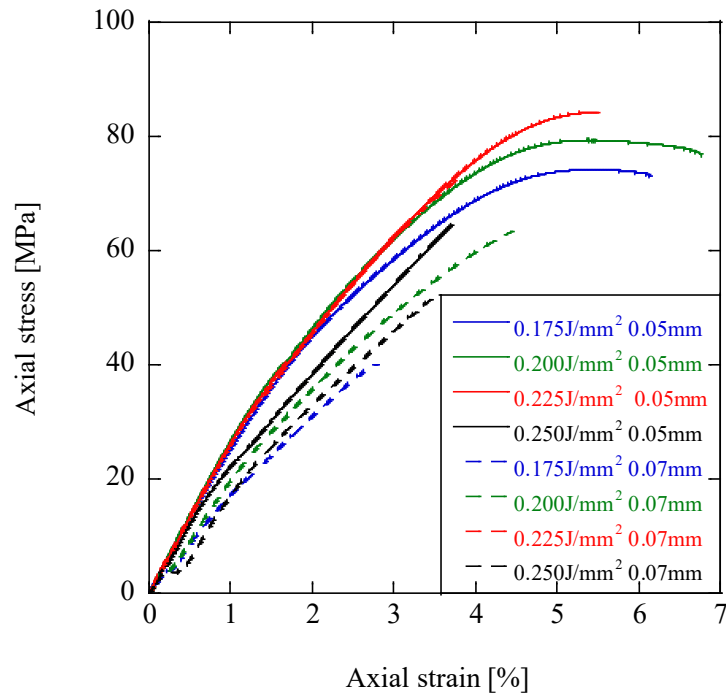


Figure 9 Stress–strain curves in powder bed temperature at 170 °C.

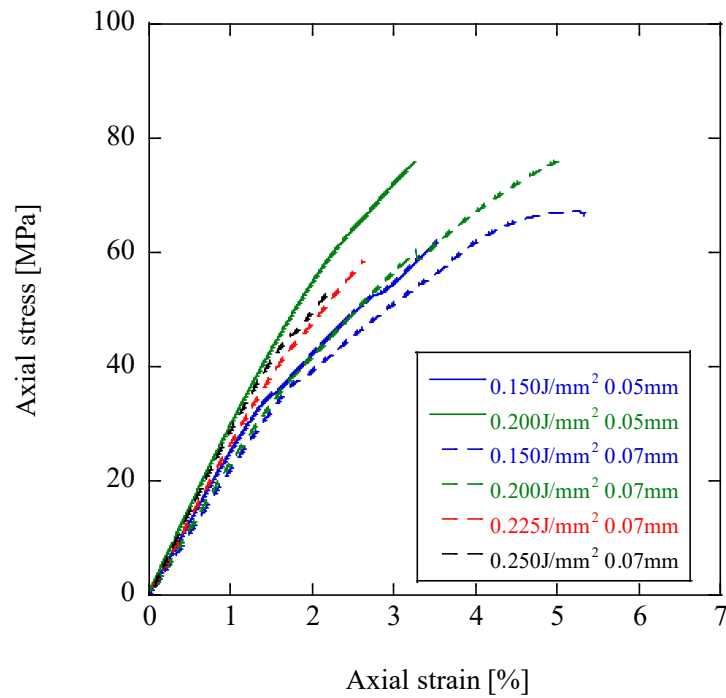


Figure 10 Stress–strain curves in powder bed temperature at 200 °C.

Cross section of specimens

Figure 11 to 14 show cross section of each specimens. Figure 11 shows specimens of layer thickness 0.05 mm and powder bed temperature 170 °C. Diagonal voids were observed in low supply energy. These diagonal voids were decreased with increasing input energy. There are few voids at the input energy 0.250 J/mm², but brown spot was observed. Figure 12 shows specimens with layer thickness 0.07 mm and powder bed temperature at 170 °C. Different tendencies from Figure 11 was shown. Diagonal voids were observed in all conditions and the size of these voids increased with increasing input energy. Figure 13 shows layer thickness 0.05 mm and powder bed temperature 200 °C and Figure 14 shows layer thickness 0.07 mm and powder bed temperature 200 °C. Diagonal voids were not observed in specimens of powder bed temperature 200 °C. Instead of diagonal voids, distorted or spherical voids were observed. Brown spots were observed in layer thickness 0.07 mm and supplied energy of 0.250 J/mm².

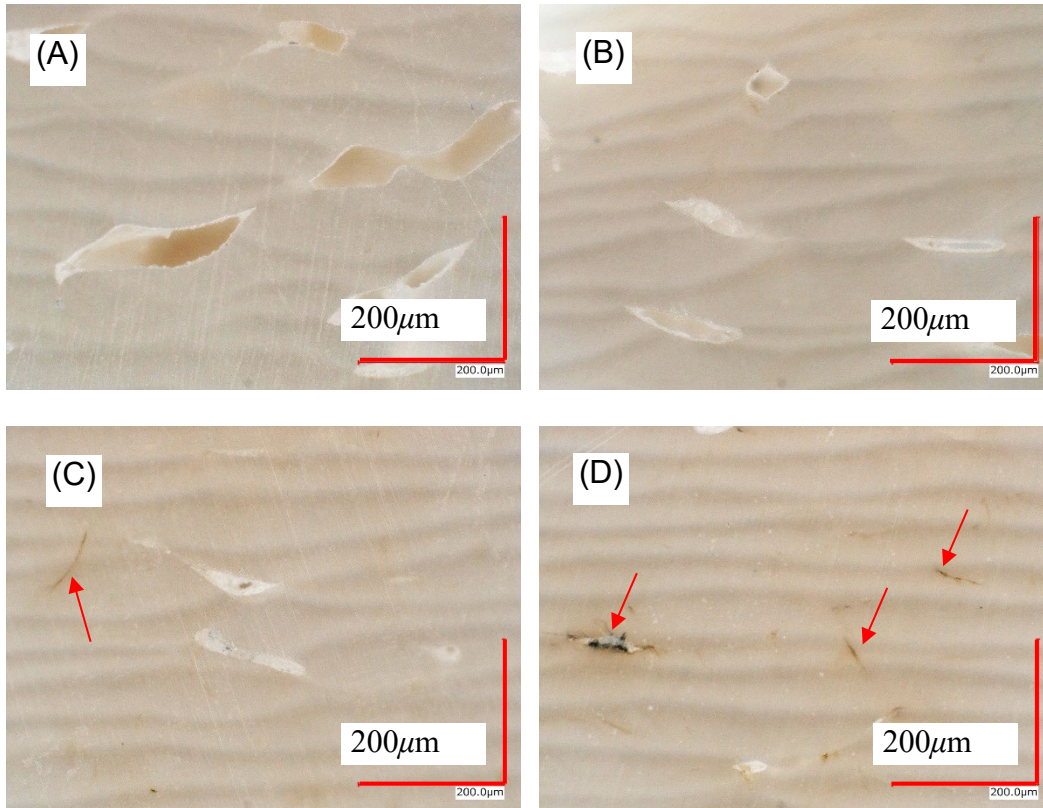


Figure 11. Cross section of specimens in powder bed temperature at 170 °C and layer thickness 0.05 mm. (A) is 175 J/mm², (B) is 200 J/mm², (C) is 225 J/mm², (D) is 250 J/mm², respectively.

Red arrows in (C), (D) indicate brown spots.

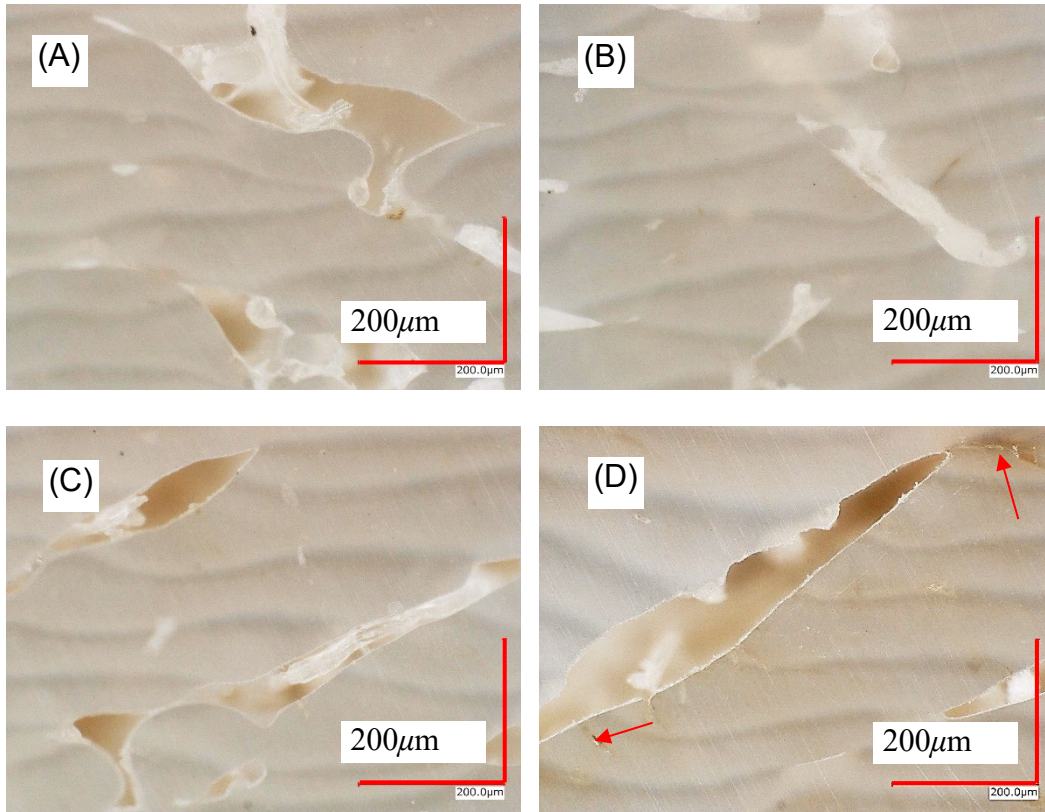


Figure 12. Cross section of specimens in powder bed temperature at 170 °C and layer thickness 0.07 mm. (A) is 175 J/mm², (B) is 200 J/mm² (C) is 225 J/mm², (D) is 250 J/mm², respectively. Red arrows in (D) indicate brown spots.

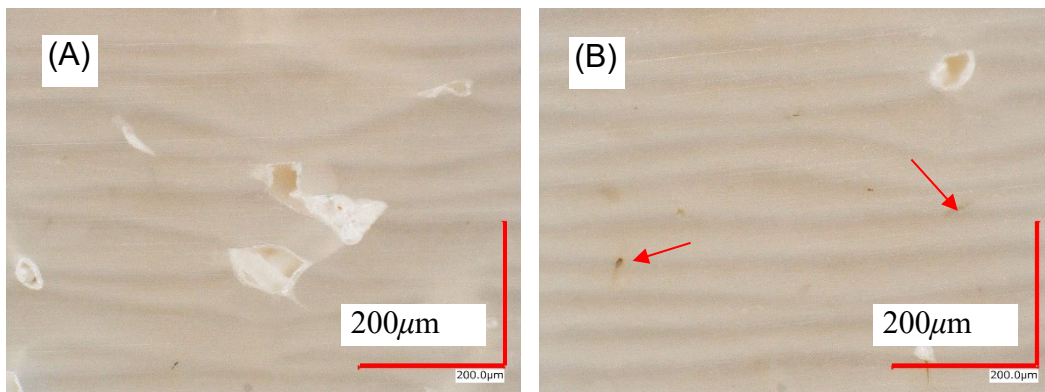


Figure 13. Cross section of specimens in powder bed temperature at 200 °C and layer thickness 0.05 mm. (A) is 150 J/mm², (B) is 200 J/mm², respectively. Red allows in (B) indicate brown spots.

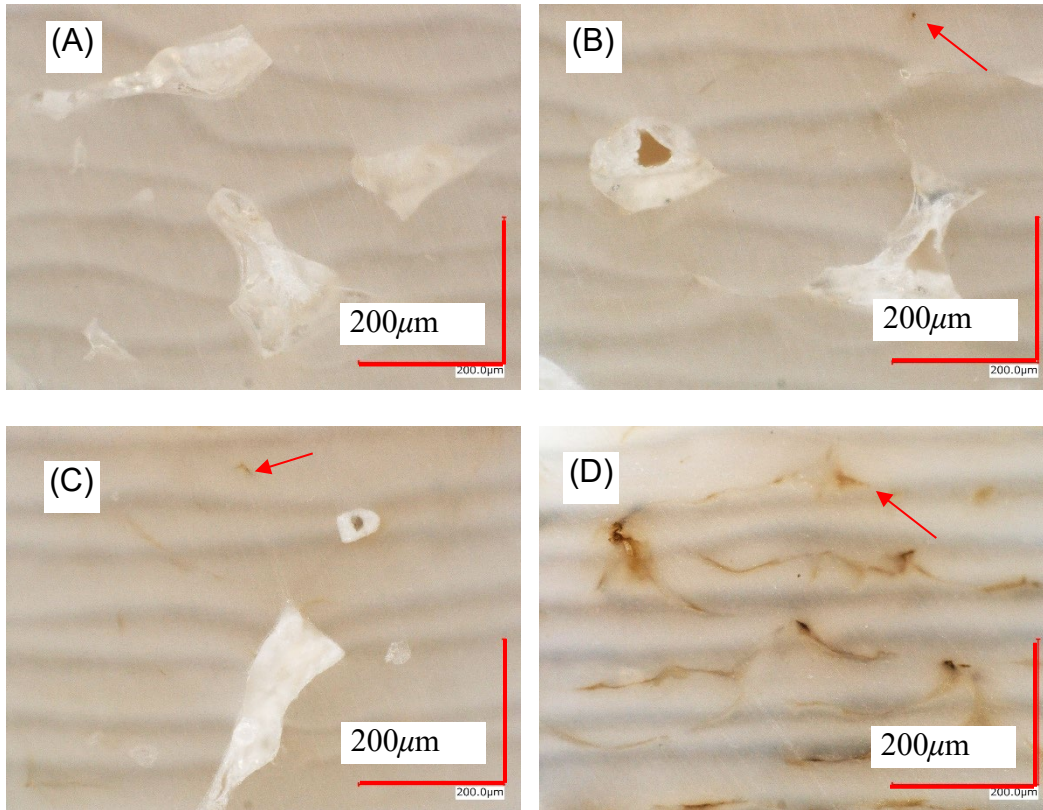


Figure 14. Cross section of specimens in powder bed temperature at 200 °C and layer thickness 0.07 mm. (A) is 150 J/mm², (B) is 200 J/mm² (C) is 225 J/mm², (D) is 250 J/mm², respectively.

Red arrows in (B), (C), (D) indicate brown spots.

Discussion

Relative density shifted higher as increasing powder bed temperature or decreasing layer thickness. The reason of this behavior is that supplied energy for melting powder layer was decreased by decreasing layer thickness or increasing powder bed temperature. High density parts such as over 95 % in relative density was obtained in powder bed temperature of 170 °C not only powder bed temperature of 200 °C reported in previous study. Furthermore, tensile strength of 80 MPa and elastic modulus of 3100 MPa were shown. These values are equivalent to previous study and it is enough as laser sintering parts. On the other hand, elongation at break was much lower than injection molded products. However, considering that the elongation at break of injection-molded PA12 exceeds 50 % and that of laser-sintered PA12 is around 10 % [11], it is thought that the elongation at break of laser-sintered PEEK is within an allowance.

From these results, it was indicated that laser sintering PEEK was successful in same temperature condition with laser sintering of PA12 by using low temperature process. As the tendency, the highest strength was not shown in the parts of highest density. This reason is the thermal degradation region was existed in the parts. Brown point in the Figure 11(D) and Figure 14(D) indicated thermal degradation regions. Thermal degradation region is brittle and works as inner crack which is start point of

break. It is known that thermal degradation of polymer causes to generation gases [10] by decomposition and discoloration. But there were not observed trace of gas generation, which is shown by exist of spherical void, only the brown spots were observed. this is assumed that thermal decomposition was occurred only powder bed surface or gases escaped during melting process from inner parts.

Stress-strain curves showed difference trends in two powder bed temperatures. this is assumed that effect of difference of crystallinity. Low crystallinity led to ductile behavior. It is indicated in previous study that crystallinity of build parts depends on powder bed temperature and lower crystallinity is shown in process of lower powder bed temperature [7].

There does not appear to be a strong correlation between strength and presence or absence of diagonal voids, but it is obvious that strength is very low for vertical load to voids. Diagonal voids were observed in lower powder bed temperature, size of diagonal voids was increased with thicker layer thickness. The reason of this phenomenon may be fused material flow and behavior of solidification. To prevent diagonal void, it is assumed from result that lower layer thickness and increasing powder bed temperature is efficiency. As the further work for stable quality, investigation of relationship between voids and layer thickness or powder bed temperature is necessary.

Conclusion

To achieve low-cost manufacturing of high-performance plastics, this study aimed to show that laser sintering of PEEK is possible on most commercially available machines by using low temperature process. The tests were performed at powder bed temperatures at 200 °C and 170 °C, and mechanical properties were measured. Parts build at a powder bed temperature of 170 °C, which is the same as the normal process of laser sintering of PA12, showed a relative density of over 95% and a tensile strength of over 80 MPa. This indicates that PEEK can be used with commercially available low powder bed temperature machines. However, there are problems to be solved such as thermal decomposition and diagonal voids, so further investigation and improvement of the process are going to perform.

Reference

- [1] S. Berretta, K.E. Evans, O.R. Ghita, "Predicting processing parameters in high temperature laser sintering (HT-LS) from powder properties" *Materials and design*, 105, 301-314(2016)
- [2] T. Wangner et al., Laser sintering of High Temperature Resistant Polymers with Carbon Black Additives, *Proceedings of the International Polymer Processing*, 19, 4, 395-401(2004)
- [3] M. Kroh, C. Bonten, P. Eyerer, "Improvement of Mechanical Properties by Additive Assisted Laser Sintering of PEEK" *Proceedings of the Polymer Processing Society 29th Annual Meeting*, (2014)
- [4] T. Hopkins, K. Dean, S. Kukureka, "Mechanical performance of PEEK produced by additive manufacturing" *Polymer testing*, 70, 511-519(2018)
- [5] P. Peyre, et al., "Experimental and numerical analysis of the selective laser sintering (SLS) of PA12 and PEKK semi-crystalline polymers", *Journal of Material Processing Technology*, 225,326-336(2015)

- [6] T. Niino, H. Haraguchi, Y. Itagaki, "Feasibility study on plastic laser sintering without powder bed preheating", proceedings of annual solid freeform fabrication symposium 2011, 17-29(2011)
- [7] T. Kigure, Y. Yamauchi, T. Niino, "Relationship between powder bed temperature and microstructure of laser sintered PA12 parts", Proceedings of annual solid freeform fabrication symposium 2019, 827-834(2019)
- [8] T. Kigure, T. Niino, "Improvement of recycle rate in laser sintering by low temperature process", proceedings of annual solid freeform fabrication symposium 2017, 550-556(2017)
- [9] T. Niino, T. Uehara, "Low temperature selective laser melting of high temperature plastic powder", Proceedings of annual solid freeform fabrication symposium 2015, 867-877(2015)
- [10] D.J.Blundell, B.N.Osborn, "The morphology of poly (aryl-ether-ether-ketone)", Polymer, 24,8, 953-958(1983)
- [11] B.V.Hooreweder et al. "On the difference in material structure and fatigue properties of nylon specimens produced by injection molding and selective laser sintering", Polymer Testing, 32, 972-981(2013)
- [12] Evonik Industries, "PRODUCT DATA", EVONIK'S PLASTIC DATABASE, <https://www.plastics-database.com/material/pdf/VESTAKEEP2000FP/VESTAKEEP2000FP>, referred on 2021/6/10